

Complex Frequency

Federico Milano, *IEEE Fellow*

Abstract—The paper introduces the concept of *complex frequency*. The imaginary part of the complex frequency is the variation with respect of a synchronous reference of the local bus frequency as commonly defined in power system studies. The real part is defined based on the variation of the voltage magnitude. The latter term is crucial for the correct interpretation and analysis of the variation of the frequency at each bus of the network. The paper also develops a set of differential equations that describe the link between complex powers and complex frequencies at network buses in transient conditions. No simplifications are assumed except for the usual approximations of the models utilized for the transient stability analysis of power systems. A variety of analytical and numerical examples show the applications and potentials of the proposed concept.

Index Terms—Power system dynamics, converter-interfaced generation, frequency control, low-inertia systems.

I. INTRODUCTION

A well-known and accepted definition of the frequency of a signal $x(t) = X_m(t) \cos(\vartheta(t))$ is given in the IEEE Std. IEC/IEEE 60255-118-1 [1], as follows:

$$f(t) = \frac{1}{2\pi} \dot{\vartheta}(t) = \frac{1}{2\pi} \dot{\theta}(t) + f_o, \quad (1)$$

where θ is the phase difference, in radians, between the angular position ϑ , also in radians, of the signal $x(t)$ and the phase due to the reference nominal frequency f_o , expressed in Hz. If the magnitude X_m of the signal is constant, this definition is adequate. However, if X_m changes with time, the definition of the frequency in (1) does not provide a meaningful way to separate the effects of the variations of ϑ and X_m . Thus, the definition of frequency in the most general conditions is a highly controversial concept that has been discussed at length in the literature (see the interesting discussion in [2] and the references therein).

This paper provides a novel interpretation of “frequency” as complex quantity, i.e., composed of a real and an imaginary part. This *complex frequency* takes into account the time dependency of both ϑ and X_m . The focus is on the theory, modeling, simulation and some application aspects of the proposed definition. The proposed complex frequency allows a neat and compact representation as well as a consistent interpretation of frequency variations in ac power systems. The complex frequency is also capable of explaining the interactions among active and reactive power injections at buses and flows in network branches. It is important to note that the proposed approach does not attempt to substitute

the modeling approaches that go beyond the classical phasor representation or that focus on analysis of non-sinusoidal signals (see, for example, [3] for a state-of-the-art survey on this topic and the several references therein). On the contrary, the proposed concept of “complex frequency” is compatible with the approaches that have been proposed in the literature as it allows interpreting angle and magnitude variations as complementary components of the same phenomenon, provided that one accepts to extend the domain of frequency to the complex numbers.

This paper focuses on electro-mechanical transients in high-voltage transmission systems. Thus, the starting point is similar to that of [4]–[7], that is, the transient conditions during which the magnitude and the phase angle of bus voltage phasors change according to the inertial response of synchronous machines and the frequency control of synchronous and non-synchronous devices. On the other hand, harmonics, unbalanced conditions and electro-magnetic transients are not taken into consideration.

The resulting formulation is *exact*, in the measure that power system models based on the dqo transform for voltage and angle stability analysis are exact; *general*, as it provides a framework to study the dynamic effect of any device on the local frequency variations at network buses; and *systematic*, because it provides with the tools to determine analytically the impact of each device on bus frequencies.

The remainder of the paper is organized as follows. Section II provides the background for the proposed theoretical framework. Section III provides the formal definition of *complex frequency* and its link with complex power injections, voltages and currents and network topology. The special cases of constant power and constant current injections as well as constant impedances are discussed in Section III-B. Section III-C discusses a variety of relevant approximated expressions that link the complex frequency to bus power injections. Section IV illustrates some applications of the analytical expressions derived in Section III to simulation, state estimation and control. Finally, Section V draws conclusions and outlines future work.

II. BACKGROUND

The starting point is the set of equations that describe the complex power injections, in per unit, at the n network buses of the system, say $\bar{s} \in \mathbb{C}^n$, as follows:

$$\bar{s}(t) = \mathbf{p}(t) + \mathbf{jq}(t) = \bar{\mathbf{v}}(t) \circ \bar{\mathbf{i}}^*(t), \quad (2)$$

where $\mathbf{p} \in \mathbb{R}^{n \times 1}$ and $\mathbf{q} \in \mathbb{R}^{n \times 1}$ are the active and reactive power injections at network buses, respectively; $\bar{\mathbf{v}} \in \mathbb{C}^{n \times 1}$ and $\bar{\mathbf{i}} \in \mathbb{C}^{n \times 1}$ are the voltages and current injections at network buses; * indicates the conjugate of a complex quantity; and \circ

F. Milano is with the School of Electrical & Electronic Engineering, University College Dublin, Belfield, Ireland. E-mail: federico.milano@ucd.ie

This work was supported by Science Foundation Ireland, by funding F. Milano under project AMPSAS, Grant No. SFI/15/IA/3074; and by the European Commission by funding F. Milano under project EdgeFLEX, Grant No. 883710.

is the Hadamard product, i.e. the element-by-element product of two vectors.¹

In steady-state, balanced conditions, (2) expresses the well-known power flow equations. However, it is important to note that, in (2), all quantities are assumed to be time dependent. The elements of the voltage and current vectors \bar{v} and \bar{i} that appears in (2), in fact, are not to be interpreted as conventional phasors, but as dynamic quantities, which in some references are called *Park's vectors* [8], [9]. A Park's vector is a complex quantity obtained from the dq-axis components of the well-known dqo transform. For example, for the voltage, one has:

$$\bar{v}(t) = v_d(t) + jv_q(t). \quad (3)$$

where the components $v_{d,k}$ and $v_{q,k}$ of the k -th element of the vector \bar{v} are calculated as follows:

$$\begin{bmatrix} v_{d,k}(t) \\ v_{q,k}(t) \\ v_{o,k}(t) \end{bmatrix} = \mathbf{P}(t) \begin{bmatrix} v_{a,k}(t) \\ v_{b,k}(t) \\ v_{c,k}(t) \end{bmatrix}, \quad (4)$$

where

$$\mathbf{P}(t) = \sqrt{\frac{2}{3}} \begin{bmatrix} \cos(\theta_o(t)) & \cos(\theta'_o(t)) & \cos(\theta''_o(t)) \\ \sin(\theta_o(t)) & \sin(\theta'_o(t)) & \sin(\theta''_o(t)) \\ \frac{1}{\sqrt{2}} & \frac{1}{\sqrt{2}} & \frac{1}{\sqrt{2}} \end{bmatrix}, \quad (5)$$

and θ_o is the angle between the phase a and the q-axis, with $\theta'_o = \omega_o$, and $\theta''_o = \theta_o - \frac{2\pi}{3}$ and $\theta'''_o = \theta_o + \frac{2\pi}{3}$. The same transformation (4) is applied to the abc currents. Since no assumption is made on the abc quantities, the d- and q-axis components of the Park's vectors \bar{v} and \bar{i} and, hence, (2) can be assumed to be valid in transient conditions. It is important to note that the reactive power is not well defined for non-sinusoidal signals.² However, it is a common assumption, which effectively underpins the vast majority of studies on the transient stability of power systems [11], to approximate the reactive power as in (2).

The $v_{o,k}$ is the o-axis or *zero* component and is null for balanced systems. If the system is not balanced and the o-axis components are not null, then the vector \mathbf{p} in (2) does not represent the total active power injections at network buses as it does not include the term $\mathbf{v}_o \circ \mathbf{i}_o$. The hypothesis of balanced system is not necessary for the developments presented below. However, since the focus is on high-voltage transmission systems, in the remainder of this paper, balanced, positive sequence operating conditions are assumed.

For the purposes of the developments given below, it is convenient to rewrite (3) in polar form:

$$\bar{v}(t) = \mathbf{v}(t) \circ \angle\boldsymbol{\theta}(t), \quad (6)$$

where $\mathbf{v} = |\bar{v}|$, $\angle\boldsymbol{\theta} = \cos(\boldsymbol{\theta}) + j\sin(\boldsymbol{\theta})$ and

$$\boldsymbol{\theta}(t) = \boldsymbol{\vartheta}(t) - \theta_o(t), \quad (7)$$

namely, $\boldsymbol{\theta}$ is the vector of bus voltage phase angles referred to the rotating dq-axis reference frame, $\boldsymbol{\vartheta}$ are the bus voltage

phase angles referred to a stationary reference and $\theta_o = \int_t \omega_o dt$ is the angle of the rotating dq-axis reference frame and ω_o is the angular frequency in rad/s of the dq-axis reference frame.

From (1), the time derivative of $\boldsymbol{\theta}$ gives:

$$\boldsymbol{\omega}(t) = \dot{\boldsymbol{\theta}}(t) = \dot{\boldsymbol{\vartheta}}(t) - \omega_o(t), \quad (8)$$

where $\boldsymbol{\omega}$ is the vector of frequency deviations with respect to the reference frequency at the network buses. In [1], it is assumed that $\omega_o = 2\pi f_o$ is constant and equal to the nominal angular frequency of the grid, e.g., $\omega_o = 2\pi 60$ rad/s in North American transmission grids. Note that ω_o being constant is not a requirement of the transform in (5). However, to carry out the derivations presented in Section III, ω_o is assumed to be constant when it is utilized to calculate the values of reactances and susceptances. As for the reactive power, this is again a widely-accepted approximation utilized in RMS models for angle and voltage stability analysis and consists in assuming that the link between current injections and voltages is given by

$$\bar{\mathbf{i}}(t) \approx \bar{\mathbf{Y}} \bar{\mathbf{v}}(t), \quad (9)$$

where $\bar{\mathbf{Y}} = \mathbf{G} + j\mathbf{B} \in \mathbb{C}^{n \times n}$ is the well-known admittance matrix of the network. It is important not to confuse (9) with the conventional relationship between current and voltage phasors (in which case (9) is an exact equality). $\bar{\mathbf{i}}$ and $\bar{\mathbf{v}}$ are Park's vectors, i.e., complex quantities with time-varying real and imaginary parts and, hence, (9) represents an approximation of the dynamics of the grid. In turn, to obtain (9), it is assumed that, for network inductances and capacitances the relationships between voltages and currents can be approximated with:

$$\begin{aligned} \bar{v} &= L\dot{\bar{i}} = L\left(\frac{d}{dt} + j\omega_o\right)\bar{i} \approx j\omega_o L\bar{i} = jX\bar{i}, \\ \bar{i} &= C\dot{\bar{v}} = C\left(\frac{d}{dt} + j\omega_o\right)\bar{v} \approx j\omega_o C\bar{v} = jB\bar{v}, \end{aligned} \quad (10)$$

where $\frac{d}{dt}$ is the time derivative relative to the Park rotating frame; $j\omega_o$ is the term due to the rotation of the Park reference; and L, C, X, B are the inductance, capacitance, reactance and susceptance, respectively. The quantities in (10) are assumed in absolute values. In turn, the approximation above assumes that electro-magnetic transients in the elements of the transmission lines and transformers are *fast* and can be assumed to be in Quasi-Steady-State (QSS). The approximation (10) is applied also to the equations of the circuits of the devices connected to the grid, e.g., the equations of the synchronous machine (see (71) in Section IV-B). The focus of this paper is, in fact, on the time scales of electro-mechanical and primary frequency and voltage control transients, which are a few orders of magnitude slower than electro-magnetic dynamics.

Merging (2) and (9) becomes:

$$\bar{\mathbf{s}}(t) = \bar{\mathbf{v}}(t) \circ [\bar{\mathbf{Y}} \bar{\mathbf{v}}(t)]^*. \quad (11)$$

These equations resemble the well-known power flow equations except for the fact that the voltages are Park's vectors, not phasors, and, hence, the power injections at buses are, in general, time-varying quantities.

¹The Hadamard product of two column vectors \mathbf{x} and \mathbf{z} can be also written as $\mathbf{x} \circ \mathbf{z} = \text{diag}(\mathbf{x}) \mathbf{z}$, where $\text{diag}(\mathbf{x})$ is a diagonal matrix whose element (i, i) is the i -th element of the vector \mathbf{x} .

²Several attempts have been done to try to overcome this issue. Among these works, we mention the monograph on the "instantaneous power theory" [10].

A. Time Derivative of Algebraic Equations

An important aspect of the developments discussed in the next section is whether (11) can be differentiated with respect to an independent variable and, in particular, with respect to time. With this aim, observe that (9) leads to the well-known QSS model for power system angle and voltage transient stability analysis, as follows [11], [12]:

$$\begin{aligned}\dot{\mathbf{x}} &= \mathbf{f}(\mathbf{x}, \mathbf{y}), \\ \mathbf{0} &= \mathbf{g}(\mathbf{x}, \mathbf{y}),\end{aligned}\quad (12)$$

where $\mathbf{f} \in \mathbb{R}^{n_x+n_y} \mapsto \mathbb{R}^{n_x}$ are the differential equations; $\mathbf{g} \in \mathbb{R}^{n_x+n_y} \mapsto \mathbb{R}^{n_y}$ are the algebraic equations, $\mathbf{x} \in \mathcal{X} \subset \mathbb{R}^{n_x}$ are the state variables; and $\mathbf{y} \in \mathcal{Y} \subset \mathbb{R}^{n_y}$ are the algebraic variables. Equations (12) are smooth in $\mathbb{R}^{n_x+n_y}$ except for a finite number of points at which discrete events occur, such as line outages and faults. In practice, these events can be modeled as *if-then* rules that modify the structure of \mathbf{f} and \mathbf{g} . There exist, of course, more sophisticated approaches to model events. These often involve the definition of additional variables and equations such as the hybrid automaton described in [13], or the approach based on Filippov theory discussed in [14]. For simplicity, however, but without lack of generality, model (12) is considered in the remainder of this work.

The implicit function theorem indicates that, if the Jacobian matrix $\partial \mathbf{g} / \partial \mathbf{y}$ is not singular, there exists a function ϕ such that:

$$\mathbf{y} = \phi(\mathbf{x}). \quad (13)$$

Equation (13) is often utilized to reduce the set of Differential-Algebraic Equations (DAEs) in (12) into a set of Ordinary Differential Equations (ODEs) that depends only on \mathbf{x} and \mathbf{z} . In this work, however, (13) is utilized the other way round, i.e., to guarantee that it is possible to define the time derivative of \mathbf{y} except for the finite number of points at which the events occur. This condition leads to:

$$\begin{aligned}\dot{\mathbf{y}} &= \frac{\partial \phi}{\partial \mathbf{x}} \dot{\mathbf{x}} = \left(\frac{\partial \mathbf{g}}{\partial \mathbf{y}} \right)^{-1} \frac{\partial \mathbf{g}}{\partial \mathbf{x}} \dot{\mathbf{x}} \\ &= \left(\frac{\partial \mathbf{g}}{\partial \mathbf{y}} \right)^{-1} \frac{\partial \mathbf{g}}{\partial \mathbf{x}} \mathbf{f}(\mathbf{x}, \phi(\mathbf{x})).\end{aligned}\quad (14)$$

The condition (14) implies that the set of DAEs in (12) is assumed to be *index 1* [15], which is the form of DAEs that describes most physical systems, including power systems [12].

The voltage magnitudes \mathbf{v} and phase angles $\boldsymbol{\theta}$ that appears in (11), and hence also the real and imaginary parts of the complex power $\bar{\mathbf{s}}$, are algebraic variables in the conventional formulation of QSS models. Thus, the assumption of index-1 DAEs allows rewriting the current injections at bus and, hence, the complex power $\bar{\mathbf{s}}$ as functions of state and discrete variables, as well as of the bus voltages $\bar{\mathbf{v}}$, namely $\bar{\mathbf{s}}(\bar{\mathbf{v}}, \mathbf{x})$, which are smooth, except at the points at which the events occur. Then, the time derivatives of $\bar{\mathbf{s}}$ can be computed with the chain rule as:

$$\dot{\bar{\mathbf{s}}} = \frac{\partial \bar{\mathbf{s}}}{\partial \bar{\mathbf{v}}} \dot{\bar{\mathbf{v}}} + \frac{\partial \bar{\mathbf{s}}}{\partial \mathbf{x}} \dot{\mathbf{x}}. \quad (15)$$

The next section of this paper elaborates on (15) and deduces an expression that involves the concept of complex frequency.

III. DERIVATION

For the sake of the derivation, it is convenient to drop the dependency on time and rewrite (11) in an element-wise notation. For a network with n buses, one has:

$$\begin{aligned}p_h &= v_h \sum_{k=1}^n v_k [G_{hk} \cos \theta_{hk} + B_{hk} \sin \theta_{hk}], \\ q_h &= v_h \sum_{k=1}^n v_k [G_{hk} \sin \theta_{hk} - B_{hk} \cos \theta_{hk}],\end{aligned}\quad (16)$$

where G_{hk} and B_{hk} are the real and imaginary parts of the element (h, k) of the network admittance matrix, i.e. $\bar{Y}_{hk} = G_{hk} + jB_{hk}$; v_h and v_k denote the voltage magnitudes at buses h and k , respectively; and $\theta_{hk} = \theta_h - \theta_k$, where θ_h and θ_k are the voltage phase angles at buses h and k , respectively. Equations (16) and all equations with subindex h in the remainder of this section are valid for $h = 1, 2, \dots, n$.

Equations (16) can be equivalently written as:

$$p_h = \sum_{k=1}^n p_{hk}, \quad \text{and} \quad q_h = \sum_{k=1}^n q_{hk}, \quad (17)$$

where

$$\begin{aligned}p_{hk} &= v_h v_k [G_{hk} \cos \theta_{hk} + B_{hk} \sin \theta_{hk}], \\ q_{hk} &= v_h v_k [G_{hk} \sin \theta_{hk} - B_{hk} \cos \theta_{hk}].\end{aligned}\quad (18)$$

Differentiating (16) and writing the active power injections as the sum of two components:

$$dp_h = \sum_{k=1}^n \frac{\partial p_h}{\partial \theta_{hk}} d\theta_{hk} + \sum_{k=1}^n \frac{\partial p_h}{\partial v_k} dv_k \equiv dp'_h + dp''_h, \quad (19)$$

In (19), dp_h is the total variation of power at bus h ; dp'_h is the quota of the active power that depends on bus voltage phase angle variations; and dp''_h is the quota of active power that depends on bus voltage magnitude variations. From (11) and using the same procedure that leads to (19), one can define two components also for the reactive power, as follows:

$$dq_h = \sum_{k=1}^n \frac{\partial q_h}{\partial \theta_{hk}} d\theta_{hk} + \sum_{k=1}^n \frac{\partial q_h}{\partial v_k} dv_k \equiv dq'_h + dq''_h. \quad (20)$$

From (17), it is relevant to observe that:

$$\frac{\partial p_h}{\partial \theta_{hk}} = -q_{hk}, \quad \text{and} \quad \frac{\partial q_h}{\partial \theta_{hk}} = p_{hk}, \quad (21)$$

which leads to rewrite dp'_h and dq'_h as:

$$\begin{aligned}dp'_h &= -\sum_{k=1}^n q_{hk} d\theta_{hk}, \\ dq'_h &= \sum_{k=1}^n p_{hk} d\theta_{hk},\end{aligned}\quad (22)$$

Recalling that $\theta_{hk} = \theta_h - \theta_k$, one has:

$$\begin{aligned}dp'_h &= -q_h d\theta_h + \sum_{k=1}^n q_{hk} d\theta_k, \\ dq'_h &= p_h d\theta_h - \sum_{k=1}^n p_{hk} d\theta_k,\end{aligned}\quad (23)$$

where the identities (17) have been used.

In the same vein, from (17), (19) and (20), dp''_h and dq''_h can be rewritten as:

$$\begin{aligned}dp''_h &= \frac{p_h}{v_h} dv_h + \sum_{k=1}^n \frac{p_{hk}}{v_k} dv_k, \\ dq''_h &= \frac{q_h}{v_h} dv_h + \sum_{k=1}^n \frac{q_{hk}}{v_k} dv_k.\end{aligned}\quad (24)$$

Let us define the quantity:

$$u_h \equiv \ln(v_h), \quad (25)$$

where both the logarithm and its argument are dimensionless. With this aim, v_h is in per unit, namely it is the ratio of two voltages (thus without units). The differential of (25) gives:

$$du_h = \frac{dv_h}{v_h}. \quad (26)$$

Then, (24) can be rewritten as:

$$\begin{aligned} dp_h'' &= p_h du_h + \sum_{k=1}^n p_{hk} du_k, \\ dq_h'' &= q_h du_h + \sum_{k=1}^n q_{hk} du_k. \end{aligned} \quad (27)$$

Equations (23) and (27) can be expressed in terms of complex powers variations:

$$\begin{aligned} d\bar{s}'_h &= dp'_h + j dq'_h = j\bar{s}_h d\theta_h - j\sum_{k=1}^n \bar{s}_{hk} d\theta_k, \\ d\bar{s}''_h &= dp''_h + j dq''_h = \bar{s}_h du_h + \sum_{k=1}^n \bar{s}_{hk} du_k, \end{aligned} \quad (28)$$

and, finally, defining the complex quantity:

$$\bar{\zeta}_h \equiv u_h + j\theta_h, \quad (29)$$

the total complex power variation is given by:

$$\begin{aligned} d\bar{s}_h &= d\bar{s}'_h + d\bar{s}''_h \\ &= dp'_h + dp''_h + j(dq'_h + dq''_h) \\ &= \bar{s}_h d\bar{\zeta}_h + \sum_{k=1}^n \bar{s}_{hk} d\bar{\zeta}_k^*. \end{aligned} \quad (30)$$

Equation (30) can be written in a compact matrix form, as follows:

$$d\bar{s} = \bar{s} \circ d\bar{\zeta} + \bar{\mathbf{S}} d\bar{\zeta}^*, \quad (31)$$

where $\bar{\mathbf{S}} \in \mathbb{C}^{n \times n}$ is a matrix whose (h, k) -th element is \bar{s}_{hk} .

The expression (31) has been obtained in general, i.e., assuming a differentiation with respect to a generic independent parameter. If this parameter is the time t , (31) can be rewritten as a set of differential equations:

$$\dot{\bar{s}} - \bar{s} \circ \bar{\eta} = \bar{\mathbf{S}} \bar{\eta}^* \quad (32)$$

where

$$\bar{\eta} = \dot{\bar{\zeta}} = \dot{\mathbf{u}} + j\dot{\boldsymbol{\theta}}, \quad (33)$$

and recalling the derivative of $\boldsymbol{\theta}$ given in (8) and defining $\boldsymbol{\varrho} \equiv \dot{\mathbf{u}}$, one obtains:

$$\bar{\eta} \equiv \boldsymbol{\varrho} + j\boldsymbol{\omega} \quad (34)$$

We define $\bar{\eta}$ as the vector of *complex frequencies* of the buses of an AC grid. Note that both real and imaginary part of (34) have, in fact, the dimension of s^{-1} , as \mathbf{u} is dimensionless and $\boldsymbol{\omega}$ is expressed in rad/s. In (34), the imaginary part is the usual angular frequency (relative to the reference ω_o). On the other hand, it is more involved to determine the physical meaning of the real part of (34), $\boldsymbol{\varrho}$. From the definition of u_h , one has $v_h = \exp(u_h)$, that is, the magnitude of the voltage is expressed as a function whose derivative is equal to the function itself. This concept is key in the theory of Lie groups and algebra, which defines the space of linear transformations of generalized ‘‘rates of change’’ [16].

Equation (32) is the sought expression of the relationship between frequency variations and power flows in an ac grid. It contains the information on how power injections of the devices connected to the grid impact on the frequency at their point of connection as well as on the rest of the grid. In (32),

the elements of \bar{s} are the inputs or *boundary conditions* at network buses and depend on the devices connected to grid, whereas $\bar{\mathbf{S}}$ depends only on network quantities.

Another way to write (32) is by splitting $\dot{\bar{s}}$ into its components $\dot{\bar{s}}'$ and $\dot{\bar{s}}''$. According the definitions of \bar{s}' and \bar{s}'' , $\dot{\bar{s}}'$ does not depend on $\boldsymbol{\varrho}$, whereas $\dot{\bar{s}}''$ does not depend on $\boldsymbol{\omega}$, as follows:

$$\begin{aligned} \dot{\bar{s}}' &= j\bar{s} \circ \boldsymbol{\omega} - j\bar{\mathbf{S}}\boldsymbol{\omega}, \\ \dot{\bar{s}}'' &= \bar{s} \circ \boldsymbol{\varrho} + \bar{\mathbf{S}}\boldsymbol{\varrho}. \end{aligned} \quad (35)$$

It is important to note that, in general, the expressions of $\dot{\bar{s}}'$ and $\dot{\bar{s}}''$ are not known *a priori*. These components, however, can be determined using (32), (35) and:

$$\dot{\bar{s}} = \dot{\bar{s}}' + \dot{\bar{s}}''. \quad (36)$$

With this regard, Section IV-B explains through an example how to calculate $\boldsymbol{\omega}$ and $\boldsymbol{\varrho}$ based on (32). In the following, (32), (35) and (36) are utilized to discuss relevant special cases.

A. Alternative Expressions

We now derive (32) in an alternative and more compact formulation as a function of the currents. First, observe that:

$$\dot{\bar{v}} = \bar{v} \circ \bar{\eta}. \quad (37)$$

The proof of (37) is given in Appendix I. Then, recalling (2), the time derivative of \bar{s} with respect to the dq-axis reference frame can be written as:

$$\begin{aligned} \dot{\bar{s}} &= \frac{d}{dt}(\bar{v} \circ \bar{i}^*) \\ &= \dot{\bar{v}} \circ \bar{i}^* + \bar{v} \circ \dot{\bar{i}}^* \\ &= \bar{v} \circ \bar{\eta} \circ \bar{i}^* + \bar{v} \circ \dot{\bar{i}}^* \\ &= \bar{s} \circ \bar{\eta} + \bar{v} \circ \dot{\bar{i}}^*, \end{aligned} \quad (38)$$

where the commutative property of the Hadamard product has been used. Substituting (38) into (32), one obtains:

$$\bar{v} \circ \dot{\bar{i}}^* = \bar{\mathbf{S}} \bar{\eta}^* \quad (39)$$

Yet another way to write (32) can be obtained by differentiating with respect of time (9), or, which is the same, dividing each row h of $\bar{\mathbf{S}}$ by the corresponding voltage \bar{v}_h in (39). Implementing this division and using (37) lead to (see also footnote 1):

$$\dot{\bar{i}} = \bar{\mathbf{Y}} [\bar{v} \circ \bar{\eta}] = \bar{\mathbf{Y}} \text{diag}(\bar{v}) \bar{\eta}, \quad (40)$$

and, defining $\bar{\mathbf{I}} = \bar{\mathbf{Y}} \text{diag}(\bar{v})$, one obtains:

$$\dot{\bar{i}} = \bar{\mathbf{I}} \bar{\eta} \quad (41)$$

As per (32), the right-hand sides of (39) and (41) depend exclusively on network quantities, whereas the left-hand side is device dependent. While equivalent, the relevant feature of (39) and (41) with respect to (32) is that the complex frequency vector only appears once.

It is worth noticing that one can also proceed the other way round, namely obtain (32) from (41). In fact, taking the conjugate of (41) and multiplying both sides by $(\bar{v} \circ)$ and using the identity (38), one re-obtains (32), as expected.

Finally, we note that (41) requires less calculations than (32). Thus, in a software tool where currents are modelled as state variables and, hence, their first time derivatives are available as a byproduct of the integration of (12), (41) can be an efficient alternative to (32) for the calculation of $\bar{\eta}$.

B. Special Cases

Three cases are considered in this section, namely, constant power injection, constant current injection, and constant admittance load. These cases illustrate the utilization of the formulas deduced above, namely (32), (39) and (41).

1) *Constant Power Injection:* We illustrate first an application of (32) for a constant power injection, say $\bar{s}_h = \bar{s}_{ho}$. From (36), the boundary condition at the h -th bus is:

$$\dot{\bar{s}}_h = 0 \quad \Rightarrow \quad \dot{\bar{s}}'_h = -\dot{\bar{s}}''_h, \quad (42)$$

and, from (35):

$$j\bar{s}_{ho}\omega_h - j\sum_{k=1}^n \bar{s}_{hk}\omega_k = -\bar{s}_{ho}\varrho_h - \sum_{k=1}^n \bar{s}_{hk}\varrho_k, \quad (43)$$

and, from (32):

$$-\bar{s}_{ho}\bar{\eta}_h = \sum_{k=1}^n \bar{s}_{hk}\bar{\eta}_k^*. \quad (44)$$

2) *Constant Admittance Load:* This case illustrates an application of (39). For a constant admittance load, the current consumption at the h -th bus is:

$$\bar{v}_h = -\bar{Y}_{ho}\bar{v}_h, \quad (45)$$

where the negative sign indicates that the current is drawn from bus h . From (39) and (45) and recalling that $\dot{v}_h = \bar{v}_h\bar{\eta}_h$ (see Appendix I), one obtains:

$$-\bar{Y}_{ho}^*v_h^2\bar{\eta}_h^* = \sum_{k=1}^n \bar{s}_{hk}\bar{\eta}_k^*. \quad (46)$$

The same result can be obtained also from (32). The power consumption at bus h can be written as:

$$\bar{s}_h = \bar{v}_h\bar{v}_h^* = -\bar{Y}_{ho}^*v_h^2, \quad (47)$$

which indicates that the power consumption \bar{s}_h in (47) does not depend on θ_h . This means that, according to (28), the term $d\bar{s}'_h = 0$ and, from (36), $\dot{\bar{s}}_h = \dot{\bar{s}}''_h$ and $\dot{\bar{s}}'_h = 0$. From the first equation of (35), one has:

$$-\bar{Y}_{ho}^*v_h^2\omega_h = \bar{s}_h\omega_h = \sum_{k=1}^n \bar{s}_{hk}\omega_k. \quad (48)$$

Then, from the time derivative of (47) and the second equation of (35), one has:

$$-2\bar{Y}_{ho}^*v_h\dot{v}_h = -\bar{Y}_{ho}^*v_h^2\varrho_h + \sum_{k=1}^n \bar{s}_{hk}\varrho_k. \quad (49)$$

Observing that, from (26), $\varrho_h = \dot{v}_h/v_h$, then:

$$v_h\dot{v}_h = v_h^2\varrho_h, \quad (50)$$

and, hence, (49) can be rewritten as:

$$-\bar{Y}_{ho}^*v_h^2\varrho_h = \bar{s}_h\varrho_h = \sum_{k=1}^n \bar{s}_{hk}\varrho_k, \quad (51)$$

The expressions (48) and (51) have the same structure and can be merged into (46). Moreover, in the summations on the right-hand-sides of (46), the term \bar{s}_{hh} is given by:

$$\bar{s}_{hh} = \bar{Y}_{hh}^*v_h^2, \quad (52)$$

and, defining $\bar{Y}_{h,\text{tot}} = \bar{Y}_{ho} + \bar{Y}_{hh}$, one obtains:

$$-\bar{Y}_{h,\text{tot}}^*v_h^2\bar{\eta}_h^* = \sum_{h \neq k}^n \bar{s}_{hk}\bar{\eta}_k^*, \quad (53)$$

which indicates that the two components of the complex frequency, ϱ_h and ω_h at the bus h of a constant admittance load are linear combinations of the ϱ_k and ω_k at the neighboring buses. This, in turn and as expected, means that constant admittance loads are *passive* devices and cannot modify the frequency at their point of connection but rather “take” the frequency that is imposed by the rest of the grid. This conclusion generalizes the results of the appendix of [7] that considers the simplified case of an admittance load connected to the rest of the system through a lossless line.

3) *Constant Current Injection:* This last example shows an application of (41). For a constant current injection, we have two cases. If the magnitude and phase angle of the current are constant, then $\dot{i}_h = 0$ and, from (41), one obtains immediately:

$$0 = \sum_{k=1}^n \bar{v}_{hk}\bar{\eta}_k, \quad (54)$$

where, \bar{v}_{hk} is the (h, k) element of $\bar{\mathbf{I}}$. Equivalently, from (39), the condition $\dot{i}_h = 0$ leads to:

$$0 = \sum_{k=1}^n \bar{s}_{hk}\bar{\eta}_k^*. \quad (55)$$

On the other hand, it is unlikely that a device is able to impose the phase angle of its current injection independently from the phase angle of its bus voltage. More likely, a device imposes a constant magnitude and power factor. In this case, the phase angle of the current will depend on the phase angle θ_h of the voltage at bus h (see Appendix II). This means that, according to (28), the term $d\bar{s}''_h = 0$ and, from (36), $\dot{\bar{s}}''_h = 0$ and $\dot{\bar{s}}_h = \dot{\bar{s}}'_h$. This result generalizes the one obtained in [17]. From (41), a current injection with constant magnitude and power factor leads to:

$$\begin{aligned} \dot{i}_h &= j\sum_{k=1}^n \bar{v}_{hk}\omega_k, \\ 0 &= \sum_{k=1}^n \bar{v}_{hk}\varrho_k, \end{aligned} \quad (56)$$

and, since the angular frequency of the current of a constant power factor load is the same of the angular frequency ω_h of the voltage at the load bus (see Appendix II and (85)), the first equation of (56) can be rewritten as:

$$\text{Re}\{\bar{\xi}_h\} = \frac{i_h}{v_h} = -j\left(\omega_h - \sum_{k=1}^n \frac{\bar{v}_{hk}}{\bar{v}_h}\omega_k\right). \quad (57)$$

C. Approximated Expressions

The mathematical developments carried out so far have assumed no simplifications except for neglecting the electromagnetic dynamics of network branches. All formulas that have been deduced are thus accurate in the measure that the effect of electro-magnetic transients are negligible. It is, however, relevant to explore whether the expressions (32), (39) and (41) can be approximated while retaining the information on the relationship between power injections and frequency variations at network buses.

Except during faults and some post-fault transients, it is not uncommon the case for which one can assume that $v_h \approx 1$ pu and that bus voltage phase angle differences are small, hence $\sin(\theta_h - \theta_k) \approx \theta_h - \theta_k$ and $\cos(\theta_h - \theta_k) \approx 1$. These

assumptions, which, in turn, are the well-known approximation utilized in the fast decoupled power flow method [18], lead to:

$$\bar{s}_{hk} \approx \bar{Y}_{hk}^* . \quad (58)$$

Equation (58) allows simplifying (32) as:

$$\dot{\bar{s}} - \bar{s} \circ \bar{\eta} \approx \bar{Y}^* \bar{\eta}^* , \quad (59)$$

and (39) and (41) as:

$$\dot{i} \approx \bar{Y} \bar{\eta} . \quad (60)$$

One can further simplify the expressions above for high-voltage transmission systems, for which $\bar{Y} \approx j\mathbf{B}$:

$$\dot{\bar{s}} - \bar{s} \circ \bar{\eta} \approx -j\mathbf{B} \bar{\eta}^* , \quad (61)$$

and (39) and (41) as:

$$\dot{i} \approx j\mathbf{B} \bar{\eta} . \quad (62)$$

Then, approximating the term $\bar{s} \circ \bar{\eta} \approx \bar{Y}_{\text{diag}}^* \bar{\eta}$, where \bar{Y}_{diag} is a matrix obtained using the diagonal elements of \bar{Y} , and splitting the real and imaginary part of $\bar{\eta}$, (61) leads to:

$$\dot{p}' \approx \mathbf{B}' \omega , \quad (63)$$

where $B'_{hk} = -B_{hk}$ and $B'_{hh} = \sum_{h \neq k}^n B_{hk}$ are the elements of \mathbf{B}' , and

$$\dot{q}'' \approx \mathbf{B}'' \varrho , \quad (64)$$

where $B''_{hk} = -B_{hk}$ and $B''_{hh} = -2B_{hh}$ are the elements of \mathbf{B}'' . Equation (63) is the expression deduced in [7] and that, with due simplifications, leads to the frequency divider formulas presented in [5].

Considering the resistive parts of the network branches, the following dual expressions hold:

$$\dot{p}'' \approx \mathbf{G}'' \varrho , \quad \dot{q}' \approx \mathbf{G}' \omega , \quad (65)$$

where the elements of \mathbf{G}' and \mathbf{G}'' are defined as $G'_{hk} = G''_{hk} = -G_{hk}$, $G'_{hh} = \sum_{h \neq k}^n G_{hk}$, and $G''_{hh} = -2G_{hh}$. Interestingly, from (65), it descends that, in lossy networks, the reactive power can be utilized to regulate the frequency.

Combining together (63), (64) and (65) leads to the following approximated expressions:

$$\dot{\bar{s}}' \approx j\bar{Y}'^* \omega , \quad \dot{\bar{s}}'' \approx \bar{Y}'' \varrho . \quad (66)$$

IV. EXAMPLES

The examples presented below apply the theory developed in the previous section and discuss applications to power system modeling, state estimation and control. In particular, three devices are discussed, namely, the synchronous machine; the voltage dependent load; and a converter-interfaced generator with frequency and voltage control capability. The objective is to illustrate the methodological approach discussed above and showcase some problems that the proposed definition of complex frequency and the expression (32) make possible to solve. In the following, all simulation results are obtained using the software tool Dome [19]. With this regard, note that, in this software tool, ω_o is set to be equal to the frequency of the Center of Inertia (CoI), nevertheless, as usually assumed in transient stability analysis, the values of reactances and susceptances are kept constant.

A. Ratio between ω and ϱ

This first example illustrates the transient behavior of the two components of the complex frequency. Figure 1 shows the transient behavior of the components of the complex frequency at a generator and a load bus, bus 2 and bus 8, respectively, for the well-known WSCC 9-bus system [11]. The estimation of ω_h and ϱ_h at the buses of the grid is obtained through a synchronous-reference frame Phase-Locked Loop (PLL) model [20]. Simulation results show that $|\omega_h| \gg |\varrho_h|$. This inequality holds for all networks and scenarios that we have tested for the preparation of this work.

It is important to note that the inequality $|\omega_h| \gg |\varrho_h|$ does not imply $\dot{\bar{s}}'_h \gg \dot{\bar{s}}''_h$. As a matter of fact, taking as an example constant impedance loads, $\dot{\bar{s}}'_h = 0$ and $\dot{\bar{s}}''_h = \dot{\bar{s}}_h$. The rationale behind this observation can be explained by rewriting (35) using (17) and an element-by-element notation:

$$\begin{aligned} \dot{\bar{s}}'_h &= j \sum_{k=1}^n \bar{s}_{hk} (\omega_h - \omega_k) , \\ \dot{\bar{s}}''_h &= \sum_{k=1}^n \bar{s}_{hk} (\varrho_h + \varrho_k) , \end{aligned} \quad (67)$$

which indicates that $\dot{\bar{s}}'_h$ is proportional to the *difference* of the elements of ω , whereas $\dot{\bar{s}}''_h$ is proportional to the *sum* of the elements of ϱ .

B. Implementation of Equation (32)

The implementation of (32) in a software tool for the simulation of power systems can be useful to determine the “exact” frequency variations at network buses in a RMS model for transient stability analysis. This topic has been discussed and solved under various hypotheses in [4]–[6]. In particular, the Frequency Divider Formula (FDF) proposed in [5] is based on (63), which is an approximation of (32).

The expression (32) states the link between the complex frequency and the rest of the variables of the system. Thus, in (32), the unknowns are $\bar{\eta}$ or, equivalently, ρ and ω . One can, of course, calculate these quantities by differentiating with respect to time u and θ , respectively. However, since u and θ are algebraic variables, (12) does not provide directly the values of their time derivatives. So either one has to use some sort of numerical differentiation (with the issues that arise at discontinuities); use some sort of estimation (e.g., the PLL utilized in the previous example); or solve (32). The latter is the approach utilized in this example.

The procedure implemented in the simulations presented in this section is as follows.

- The system variables x and y are initialized using (12).
- The DAEs defined by (12) are integrated using a conventional numerical scheme (in this case, the implicit trapezoidal method with fixed time step).
- Discrete events are also handled with a conventional approach. Specifically, an approach based on *if-then* rules that switch the equations on the right-hand-side of (12) has been utilized.
- Finally, (32) – or, alternatively, (39) or (41) – and the values x , y and \dot{x} obtained at each step of the time

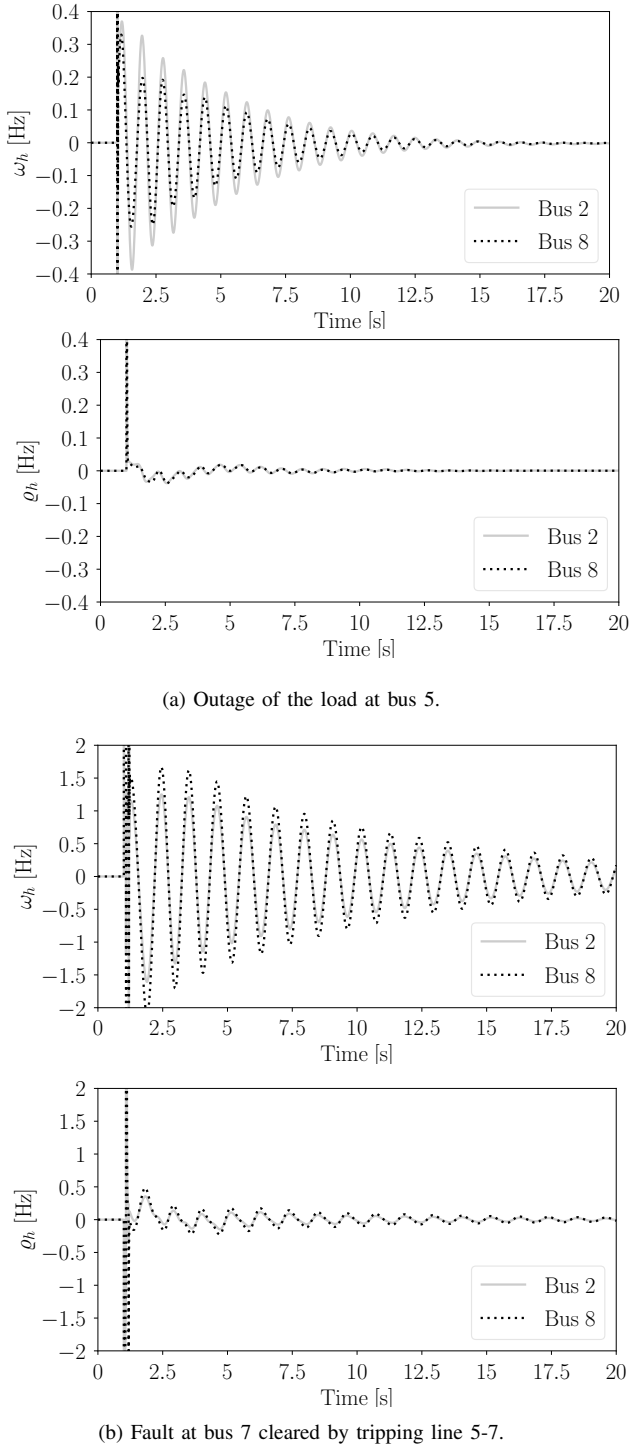


Fig. 1: Transient behavior of the components of the complex frequency for the WSCC 9-bus system.

domain integration are utilized to calculate $\bar{\eta}$.³

With regard to the last step, i.e., the determination of $\bar{\eta}$, note that (32) can be rewritten as a set of $2n$ real equations, with unknowns (ϱ, ω) . The right-hand side of (32) is linear with

³The procedure described above is an open-loop, i.e., (32) are solved “off-line” based on the solution obtained by integrating (12). In a closed loop, i.e., if the elements of the complex frequency are utilized as inputs to some controllers or one wants to take into account the dependence on the frequency in the model of a device, then (12) has to be extended to include (32).

respect to $\bar{\eta}$, so it remains to determine the dependency of the elements of $\bar{s} - \bar{s} \circ \bar{\eta}^*$ – or, alternatively, of $\bar{v} \circ \dot{i}^*$ from (39) or \dot{i} from (41) – on $\bar{\eta}$ and, eventually, on the time derivatives of the state variables \dot{x} .

We illustrate the procedure using a conventional 4th order model of the synchronous machine and (32). The stator voltage of the machine with respect to its dq-axis reference frame is linked to the grid voltage v_h with the following equations [11]:

$$\bar{v}_s = v_{s,d} + jv_{s,q} = \bar{v}_h \angle \left(\frac{\pi}{2} - \delta_r \right), \quad (68)$$

where δ_r is the rotor angle of the machine. The time derivative of (68) gives (see Appendix I for the derivative of \bar{v}_h):

$$\dot{\bar{v}}_s = \bar{v}_s (\bar{\eta}_h - j\omega_r), \quad (69)$$

where ω_r is the deviation in rad/s of the angular speed of the machine with respect to ω_o . The real and imaginary terms of (69) can be written as:

$$\begin{aligned} \dot{v}_{s,d} &= v_{s,d}\varrho_h - v_{s,q}\omega_h + v_{s,q}\omega_r, \\ \dot{v}_{s,q} &= v_{s,q}\varrho_h + v_{s,d}\omega_h - v_{s,d}\omega_r. \end{aligned} \quad (70)$$

Then, the stator electrical and magnetic equations are:

$$\begin{aligned} X'_d i_{s,d} + R_a i_{s,q} &= -v_{s,q} + e'_{r,q} \\ R_a i_{s,d} - X'_q i_{s,q} &= -v_{s,d} + e'_{r,d} \end{aligned} \quad (71)$$

where $\bar{i}_s = i_{s,d} + j i_{s,q}$ is the stator current. From (71), one can thus obtain the expressions of $i_{s,d}$ and $i_{s,q}$ as a function of $v_{s,d}$, $v_{s,q}$ and the state variables $e'_{r,d}$ and $e'_{r,q}$. In this case, these relationships are linear, so, one can obtain the current explicitly as:

$$\begin{bmatrix} i_{s,d} \\ i_{s,q} \end{bmatrix} = \begin{bmatrix} X'_d & R_a \\ R_a & -X'_q \end{bmatrix}^{-1} \begin{bmatrix} -v_{s,q} + e'_{r,q} \\ -v_{s,d} + e'_{r,d} \end{bmatrix}, \quad (72)$$

or, equivalently:

$$\begin{aligned} i_{s,d} &= k_{v,dd}v_{s,d} + k_{v,dq}v_{s,q} + k_{e,dd}e'_{r,d} + k_{e,dq}e'_{r,q}, \\ i_{s,q} &= k_{v,qd}v_{s,d} + k_{v,qq}v_{s,q} + k_{e,qd}e'_{r,d} + k_{e,qq}e'_{r,q}, \end{aligned} \quad (73)$$

where the k -coefficients are constant and depend on R_a , X'_d and X'_q . Differentiating (73) with respect to time, substituting the expressions of $\dot{v}_{s,d}$ and $\dot{v}_{s,q}$ from (70) and applying the chain rule, the time derivatives of the components of the current can be written in the form:

$$\begin{aligned} \dot{i}_{s,d} &= \frac{\partial i_{s,d}}{\partial \varrho_h} \varrho_h + \frac{\partial i_{s,d}}{\partial \omega_h} \omega_h + \frac{\partial i_{s,d}}{\partial \omega_r} \omega_r + \frac{\partial i_{s,d}}{\partial e'_{r,d}} \dot{e}'_{r,d} + \frac{\partial i_{s,d}}{\partial e'_{r,q}} \dot{e}'_{r,q}, \\ \dot{i}_{s,q} &= \frac{\partial i_{s,q}}{\partial \varrho_h} \varrho_h + \frac{\partial i_{s,q}}{\partial \omega_h} \omega_h + \frac{\partial i_{s,q}}{\partial \omega_r} \omega_r + \frac{\partial i_{s,q}}{\partial e'_{r,d}} \dot{e}'_{r,d} + \frac{\partial i_{s,q}}{\partial e'_{r,q}} \dot{e}'_{r,q}, \end{aligned} \quad (74)$$

where, in the right-hand side, ϱ_h and ω_h are unknown and all other variables and terms are calculated based on the current solution of (12). Then, from (39), one obtains:

$$\begin{aligned} \text{Re}\{\bar{v}_h \dot{i}_h^*\} &= \text{Re}\{\bar{v}_s \dot{i}_s^*\} = v_{s,d}\dot{i}_{s,d} + v_{s,q}\dot{i}_{s,q}, \\ \text{Im}\{\bar{v}_h \dot{i}_h^*\} &= \text{Im}\{\bar{v}_s \dot{i}_s^*\} = v_{s,q}\dot{i}_{s,d} - v_{s,d}\dot{i}_{s,q}. \end{aligned} \quad (75)$$

Finally, substituting (74) into (75), one obtains the expressions of the left-hand side of (39) at the buses of the synchronous machines.

The very same procedure can be applied to any device of the grid and, in the vast majority of the cases, the resulting expressions are linear with respect to (ϱ, ω) . Hence, at each

time step of a time domain simulation one need to solve a problem of the type $\mathbf{A}\chi = \mathbf{b}$, where $\chi = [\varrho^T, \omega^T]^T$, and:

$$\mathbf{A} = \begin{bmatrix} [\mathbf{H} + \text{diag}(\mathbf{p}) - \mathbf{P}_\varrho] & [\mathbf{K} - \text{diag}(\mathbf{q}) - \mathbf{P}_\omega] \\ [\mathbf{K} + \text{diag}(\mathbf{q}) - \mathbf{Q}_\varrho] & -[\mathbf{H} - \text{diag}(\mathbf{p}) + \mathbf{Q}_\omega] \end{bmatrix} \quad (76)$$

and

$$\mathbf{b} = \begin{bmatrix} \mathbf{P}_x \dot{\mathbf{x}} \\ \mathbf{Q}_x \dot{\mathbf{x}} \end{bmatrix}, \quad (77)$$

where $\mathbf{H} = \text{Re}\{\bar{\mathbf{S}}\}$ and $\mathbf{K} = \text{Im}\{\bar{\mathbf{S}}\}$; \mathbf{P}_ϱ , \mathbf{P}_ω , \mathbf{Q}_ϱ and \mathbf{Q}_ω are the Jacobian $n \times n$ matrices of \mathbf{p} and \mathbf{q} with respect to ϱ and ω , respectively; and \mathbf{P}_x and \mathbf{Q}_x are the Jacobian $n \times n_x$ matrices of \mathbf{p} and \mathbf{q} with respect to the state variables \mathbf{x} , respectively.

Figure 2 shows the imaginary part of the complex frequency as obtained for the WSCC 9-bus system using a 4th and a 2nd order model of the synchronous machines, as well as for a scenario where the machine at bus 3 is substituted for a Converter-Interfaced Generator (CIG). The model of the CIG is shown in Fig. 3. The results obtained using PLLs matches well the “exact” results obtained with proposed method (indicated with CF in the legends) except for the numerical spikes that following the load disconnection and a small delay that is due to the control loop of the PLL. The proposed formula is also robust with respect to noise as shown in Fig. 2b.

The events create spikes in the estimation of ω obtained with the PLL. The behavior of ω as estimated with the complex frequency, on the other hand, depends on the dynamics of the device connected to the bus where the frequency is estimated. It is smooth for the 2nd order synchronous machine and show a small jump for the 4th order synchronous machine. The latter behavior is due to the dependence of the frequency on the voltage magnitude, which is modeled as an algebraic variable in (12). On the other hand, the behavior of the ω estimated with the complex frequency at the CIG bus shows a relatively fast transient after the load disconnection (see Fig. 2d). This is due to the dynamics of the currents of the converter.

Figure 2 also shows the results obtained using the FDF proposed in [5]. The FDF matches closely the results of the proposed method when considering the simplified 2nd order model of the machines but introduces some errors if the machine model includes rotor flux dynamics or when considering the CIG.

C. Voltage Dependent Load (VDL)

The power consumption of a VDL is:

$$\bar{s}_h = p_h + jq_h = -p_o v_h^{\gamma_p} - j q_o v_h^{\gamma_q}, \quad (78)$$

then:

$$\begin{aligned} \dot{\bar{s}}_h &= -p_o \gamma_p \dot{v}_h v_h^{\gamma_p-1} - j q_o \gamma_q \dot{v}_h v_h^{\gamma_q-1} \\ &= (\gamma_p p_h + j \gamma_q q_h) \varrho_h, \end{aligned} \quad (79)$$

where it has been assumed that the exponents γ_p and γ_q are constant and that p_o and q_o vary “slowly” with respect to v_h . If $\gamma_p = \gamma_q = \gamma$, then $\dot{\bar{s}}_h = \gamma \bar{s}_h \varrho_h$, which generalizes the results obtained in Section III-B.2.

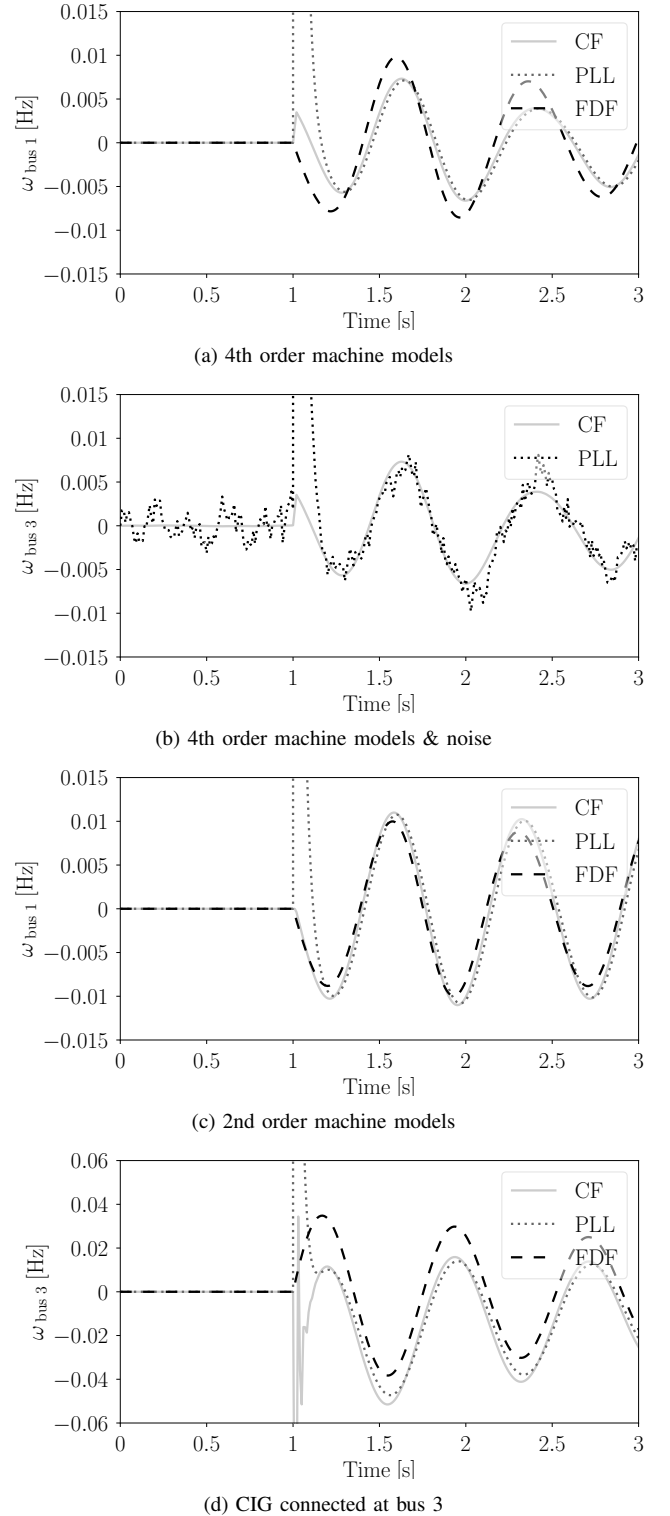


Fig. 2: Comparison of bus frequencies using PLL, FDF and the proposed approach based on the complex frequency. The plots refers to the WSCC 9-bus system following the disconnection at $t = 1$ s of the load at bus 5.

As an application, we utilize (79) to estimate the parameters γ_p and γ_q of a VDL using a similar technique as the one proposed in [17]. From (32) and (79), one obtains:

$$(\gamma_p p_h + j \gamma_q q_h) \varrho_h = \sum_{k=1}^n [\bar{s}_{hk} (\bar{\eta}_h + \bar{\eta}_k^*)], \quad (80)$$

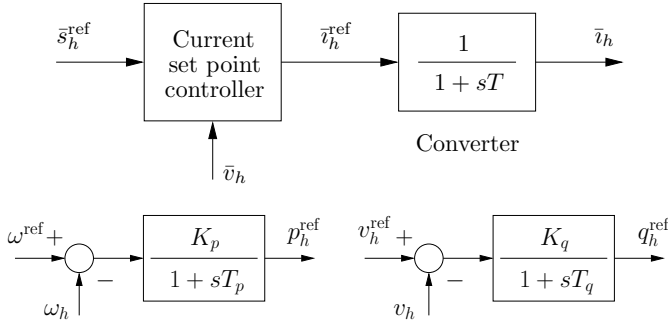


Fig. 3: Simplified scheme of a CIG and its controllers.

and, splitting real and imaginary parts:

$$\begin{aligned} \gamma_p &= (p_h \varrho_h)^{-1} \text{Re} \left\{ \sum_{k=1}^n \bar{s}_{hk} (\bar{\eta}_h + \bar{\eta}_k^*) \right\}, \\ \gamma_q &= (q_h \varrho_h)^{-1} \text{Im} \left\{ \sum_{k=1}^n \bar{s}_{hk} (\bar{\eta}_h + \bar{\eta}_k^*) \right\}, \end{aligned} \quad (81)$$

where the right-hand sides can be determined based on measurements. The fact that $\varrho_h \rightarrow 0$ in steady-state can create numerical issues, which can be solved, as discussed in [17], using finite differences over a period of time Δt , namely $\bar{\eta}_h \approx \Delta \bar{\zeta}_h / \Delta t$, $\bar{\eta}_k^* \approx \Delta \bar{\zeta}_k^* / \Delta t$, and $\varrho_h \approx \Delta u_h / \Delta t$, as follows:

$$\begin{aligned} \hat{\gamma}_p &\approx (p_h \Delta u_h)^{-1} \text{Re} \left\{ \sum_{k=1}^n \bar{s}_{hk} (\Delta \bar{\zeta}_h + \Delta \bar{\zeta}_k^*) \right\}, \\ \hat{\gamma}_q &\approx (q_h \Delta u_h)^{-1} \text{Im} \left\{ \sum_{k=1}^n \bar{s}_{hk} (\Delta \bar{\zeta}_h + \Delta \bar{\zeta}_k^*) \right\}. \end{aligned} \quad (82)$$

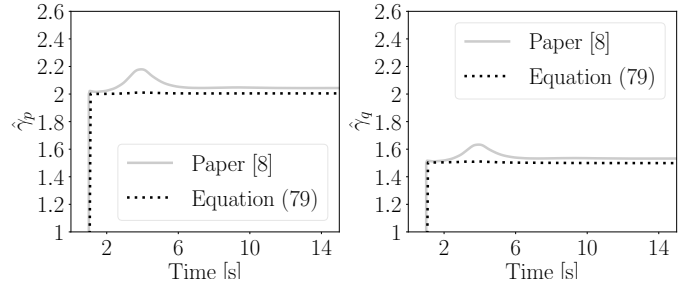
Equations (81) and (82) generalize the empirical formulas to estimate γ_p and γ_q proposed in [17]. The latter, in fact, can be obtained from (82) by approximating $\bar{s}_{hk} \approx -jB_{hk}$.

Figure 4 shows the results obtained for the WSCC 9-bus system where the bus connected at bus 8 is a VDL with $\gamma_p = 2$ and $\gamma_q = 1.5$. The results show that (82) is, as expected, more precise than the approximated estimations based on the expression proposed in [17]. Equation (82) is, in fact, an exact expression and its accuracy depends exclusively on the accuracy of the measurements of $\bar{\zeta}_h$ and $\bar{\zeta}_k$, which can be obtained, for example, with PMUs. If the R/X ratio of the transmission lines of the system is changed to resemble that of a distribution system, (82) appears also numerically more robust than its approximated counterparts (see Fig. 4b).

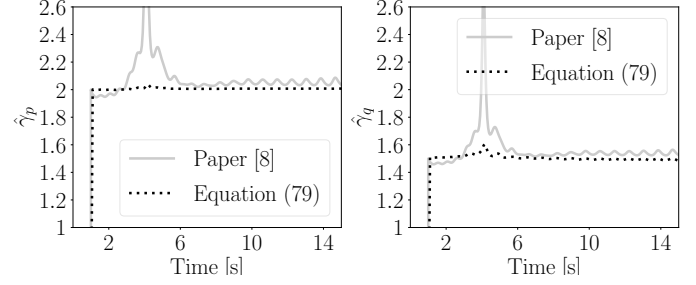
D. Converter-Interfaced Generation

This last example illustrates an application of the approximated expression (65). We focus in particular on the link between ω and \dot{q} through the resistances of network branches. Using again the WSCC 9-bus system and substituting two synchronous machines with CIGs, we compare the dynamic response of the system following a load variation using the control scheme of Fig. 3 (Control 1), and the control scheme shown in Fig. 5 (Control 2). The latter regulates the frequency by both the active and reactive powers of the CIGs.

Figure 6 shows that Control 2 is more effective than Control 1 to reduce the variations of the frequency. This result indicates that the relationship between q and ω is not weak and can be exploited to improve the frequency response of low-inertia systems. This result is predicted by (65) and hence by (32).



(a) Ratio of transmission lines: $R/X \ll 1$.



(b) Ratio of transmission lines: $R/X \approx 1$.

Fig. 4: Estimation of the exponents of the VDL connected at bus 8 following the disconnection of 15% of the load at bus 5 at $t = 1$ s for the WSCC 9-bus system.

The simplified converter-interfaced generator model shown in Fig. 5, with differential equations:

$$\begin{aligned} T_p \dot{p}_h &= K_p (\omega^{\text{ref}} - \omega_h) - p_h, \\ T_q \dot{q}_h &= K_q (v^{\text{ref}} - v_h) - q_h. \end{aligned} \quad (83)$$

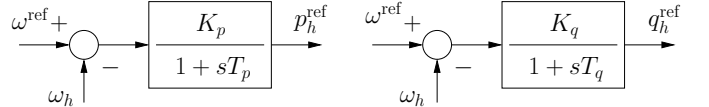


Fig. 5: Alternative frequency control through active and reactive powers for the CIG of Fig. 3.

V. CONCLUSIONS

The paper introduces a new physical quantity, namely, the *complex frequency*. This quantity allows writing the differential of power flow equations in terms of complex powers and voltages at network buses. The most significant property of the newly defined complex frequency is its ability to give a more robust and clean indication of frequency than what generally accepted in the literature, especially to describe the behavior of the frequency at buses close to a disturbance. For example, it is well known that many other methods result in meaningless spikes in frequency at the inception and clearing of faults and other sudden disturbances. The proposed definition provides a solution to this issue.

The proposed definition of complex frequency is in accordance with the commonly accepted definition of frequency and generalizes it. In fact, if the magnitude of the voltage is constant, then $\rho = 0$ and the magnitude of the complex frequency

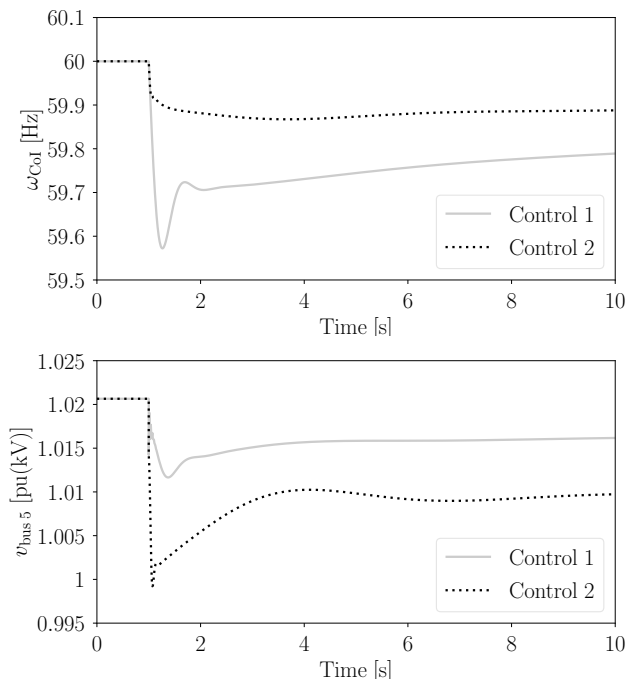


Fig. 6: Frequency of the CoI and voltage at bus 5 following the connection of $p = 0.25$ pu at bus 5 at $t = 1$ s for the WSCC 9-bus system with high penetration of CIG.

coincides with (1). The common definition of frequency is thus a special case of the complex frequency. On the other hand, if the magnitude of the voltage is not constant, then, the complex frequency extends the concept of frequency by including an additional term, ρ .

Then, the paper shows how the complex frequencies are related to the time derivatives of the voltages and to the power/current injections at the network buses. In this vein, noteworthy expressions are (32), (39) and (41). It is also shown that these expressions are a generalization of the FDF proposed in [5].

The proposed framework can be used, for example, for evaluating how good is the estimation of the frequency obtained with a PLL and also appears as an useful tool to design novel and efficient controllers. The several analytical and numerical examples discussed in Sections III and IV show the prospective applications of the proposed theoretical approach. The newly introduced term ρ can be also expected to have practical applications. An example is given in Section IV-C.

Future work will focus on further elaborating the expression (32) and exploiting its features for the control and state estimation of power systems. A relevant question worth of further study is how to take into account fast dynamics, such as transmission line dynamics, in the evaluation of the complex frequency. It appears relevant also to combine the proposed complex frequency approach to some of the techniques described in [3]. Particularly interesting, for example, is the “beyond-phasor” approach based on the Hilbert transform proposed in [21].

APPENDIX I TIME-DERIVATIVE OF THE VOLTAGE

This appendix provides the proof of (37). With this aim, let us consider the h -th element of (37), namely $\bar{v}_h = v_h \angle \theta_h = v_h (\cos \theta_h + j \sin \theta_h)$. The time derivative of \bar{v}_h with respect to the dq-axis reference frame gives:

$$\begin{aligned} \dot{\bar{v}}_h &= \dot{v}_h \angle \theta_h + j v_h \omega_h \angle \theta_h \\ &= v_h (\dot{\rho}_h \angle \theta_h + j \omega_h \angle \theta_h) \\ &= v_h \angle \theta_h (\dot{\rho}_h + j \omega_h) \\ &= \bar{v}_h \bar{\eta}_h, \end{aligned}$$

where the following identities hold:

$$\begin{aligned} \frac{d}{dt} \angle \theta_h &= \omega_h (-\sin \theta_h + j \cos \theta_h) \\ &= j \omega_h (\cos \theta_h + j \sin \theta_h) \\ &= j \omega_h \angle \theta_h. \end{aligned}$$

APPENDIX II COMPLEX FREQUENCY OF CURRENT INJECTIONS

Let us assume that $\bar{i}_h = i_h \angle \beta_h$, then, one has:

$$\dot{\bar{i}}_h = \bar{i}_h \left(\frac{\dot{i}_h}{i_h} + j \dot{\beta}_h \right) = \bar{i}_h \bar{\xi}_h, \quad (84)$$

where $\bar{\xi}_h$ is the complex frequency of the current injection at bus h which is determined using the same procedure that leads to (37) and that is described in the Appendix.

A relevant special case is that of constant power factor devices (either generators or loads), for which $\beta_h = \theta_h + \varphi_{ho}$, where φ_{ho} is the constant power factor angle. Then:

$$\dot{\beta}_h = \dot{\theta}_h + \dot{\varphi}_{ho} = \omega_h. \quad (85)$$

On the other hand, $\text{Re}\{\bar{\xi}_h\} = \rho_h$ only if $i_h = k v_h$. Since a constant impedance has constant power factor and its current is proportional to the voltage, it satisfies the condition $\bar{\xi}_h = \bar{\eta}_h$, $\forall t$.

ACKNOWLEDGMENTS

The author wishes to thank Dr. Ioannis Dassios, University College Dublin, for carefully revising the mathematical derivations given in the paper.

REFERENCES

- [1] “IEEE/IEC International Standard - Measuring relays and protection equipment - Part 118-1: Synchrophasor for power systems - Measurements,” pp. 1–78, 2018.
- [2] H. Kirkham, W. Dickerson, and A. Phadke, “Defining power system frequency,” in *IEEE PES General Meeting*, 2018, pp. 1–5.
- [3] M. Paolone, T. Gaunt, X. Guillaud, M. Liserre, S. Meliopoulos, A. Monti, T. Van Cutsem, V. Vittal, and C. Vourmas, “Fundamentals of power systems modelling in the presence of converter-interfaced generation,” *Electric Power Systems Research*, vol. 189, p. 106811, 2020.
- [4] J. Nutaro and V. Protopopescu, “Calculating frequency at loads in simulations of electro-mechanical transients,” *IEEE Trans. on Smart Grid*, vol. 3, no. 1, pp. 233–240, 2012.
- [5] F. Milano and Á. Ortega, “Frequency divider,” *IEEE Trans. on Power Systems*, vol. 32, no. 2, pp. 1493–1501, 2017.
- [6] H. Golpîra and A. R. Messina, “A center-of-gravity-based approach to estimate slow power and frequency variations,” *IEEE Trans. on Power Systems*, vol. 33, no. 1, pp. 1026–1035, 2018.

- [7] F. Milano and Á. Ortega, "A method for evaluating frequency regulation in an electrical grid Part I: Theory," *IEEE Trans. on Power Systems*, 2020, in press.
- [8] F. Saccomanno, *Electric Power Systems - Analysis and Control*. New York: John Wiley & Sons, 2003.
- [9] F. Milano and Á. Ortega, *Frequency Variations in Power Systems: Modeling, State Estimation, and Control*. Hoboken, NJ: Wiley, 2020.
- [10] H. Akagi, E. H. Watanabe, and M. Aredes, *Instantaneous Power Theory and Applications to Power Conditioning*, 2nd ed. New York: Wiley IEEE Press, 2017.
- [11] P. W. Sauer and M. A. Pai, *Power System Dynamics and Stability*. Upper Saddle River, NJ: Prentice Hall, 1998.
- [12] F. Milano, *Power System Modelling and Scripting*. London, UK: Springer, 2010.
- [13] I. Hiskens, "Power system modeling for inverse problems," *IEEE Transactions on Circuits and Systems I: Regular Papers*, vol. 51, no. 3, pp. 539–551, 2004.
- [14] M. A. A. Murad, M. Liu, and F. Milano, "Modeling and simulation of variable limits on conditional anti-windup pi controllers for vsc-based devices," *IEEE Transactions on Circuits and Systems I: Regular Papers*, vol. 68, no. 7, pp. 3079–3088, 2021.
- [15] U. M. Ascher and L. R. Petzold, *Computer Methods for Ordinary Differential Equations and Differential-Algebraic Equations*, 1st ed. USA: Society for Industrial and Applied Mathematics, 1998.
- [16] H. Stephani, *Differential Equations: Their Solution Using Symmetries*, M. MacCallum, Ed. Cambridge University Press, 1990.
- [17] Á. Ortega and F. Milano, "Estimation of voltage dependent load models through power and frequency measurements," *IEEE Trans. on Power Systems*, vol. 35, no. 4, pp. 3308–3311, 2020.
- [18] B. Stott and O. Alsac, "Fast decoupled load flow," *IEEE Trans. on Power Systems*, vol. PAS-93, no. 3, pp. 859–869, 1974.
- [19] F. Milano, "A Python-based software tool for power system analysis," in *IEEE PES General Meeting*, 2013, pp. 1–5.
- [20] Á. Ortega and F. Milano, "Comparison of different PLL implementations for frequency estimation and control," in *ICHQP*, 2018, pp. 1–6.
- [21] A. Derviškić, G. Frigo, and M. Paolone, "Beyond phasors: Modeling of power system signals using the hilbert transform," *IEEE Transactions on Power Systems*, vol. 35, no. 4, pp. 2971–2980, 2020.



Federico Milano (F'16) received from the University of Genoa, Italy, the M.E. and Ph.D. in Electrical Engineering in 1999 and 2003, respectively. From 2001 to 2002, he was with the Univ. of Waterloo, Canada. From 2003 to 2013, he was with the Univ. of Castilla-La Mancha, Spain. In 2013, he joined the Univ. College Dublin, Ireland, where he is currently Professor of Power Systems Control and Protections and Head of Electrical Engineering. His research interests include power systems modeling, control and stability analysis.